

RESEARCH

Open Access



Mechanism study of YangJing ZhongYu decoction on regulating mitochondrial dynamics of ovarian granular cells and improving diminished ovarian reserve

Ping Li¹ and Jilin Kuang^{1*}

Abstract

Objective Diminished ovarian reserve (DOR) encompasses both reproductive and endocrine disorders, resulting in a decline in female fertility. This paper explored the mechanism of Yangjing Zhongyu Decoction (YJZYD) regulating mitochondrial dynamics of ovarian granulosa cells (GCs) to improve DOR.

Methods DOR patients were treated with YJZYD, with ovarian volume (OV), antral follicle count (AFC), and endometrial thickness (EMT) detected. C57BL/6 female mice were treated by cyclophosphamide (Cy) intraperitoneal injection and YJZYD solution daily gavage, with serum anti-Mullerian hormone (AMH), follicle-stimulating hormone (FSH), luteinizing hormone (LH), and estradiol (E2) levels determined. Ovarian GCs (KGN) were interfered with 4-Hydroperoxy-Cyclophosphamide (4-HC) and treated with the MAPK/ERK pathway inhibitor or activator.

Results DOR patients showed increased levels of serum AMH, E2, OV, AFC and EMT, while reduced FSH and LH levels after YJZYD treatment. After Cy induction, DOR mice exhibited irregular estrous cycles, diminished serum AMH and E2 levels, elevated FSH and LH levels, reduced follicle number and atresia follicle number, disorderly arranged GCs, and severe interstitial fibrosis. After 4-HC treatment, KGN proliferation and Bcl-2, MFN1, and MFN2 were suppressed, while apoptotic rate, Bax, Cleaved-caspase-3, and p-Drp1 (Ser616) levels, and mitochondrial fission and quantity increased. YJZYD promoted 4-HC-treated KGN proliferation, boosted mitochondrial fusion, and inhibited apoptosis and mitochondrial fission via the MAPK/ERK pathway.

Conclusion YJZYD promoted ovarian GC proliferation and mitochondrial fusion, suppressed cell apoptosis and mitochondrial fission, and effectively improved DOR in mice by activating the MAPK/ERK pathway, providing a theoretical basis for the clinical application value of YJZYD in DOR treatment.

Keywords YangJing zhongyu decoction, Diminished ovarian reserve, Ovarian granulosa cells, Mitochondrial dynamics, Proliferation, Apoptosis

*Correspondence:

Jilin Kuang
JilinKuang0721@163.com

¹Department of Gynecology, The Second Affiliated Hospital of Hunan University of Chinese Medicine, 233 CAI'e North Road, Kaifu District, Changsha 410005, Hunan, China



© The Author(s) 2024. **Open Access** This article is licensed under a Creative Commons Attribution-NonCommercial-NoDerivatives 4.0 International License, which permits any non-commercial use, sharing, distribution and reproduction in any medium or format, as long as you give appropriate credit to the original author(s) and the source, provide a link to the Creative Commons licence, and indicate if you modified the licensed material. You do not have permission under this licence to share adapted material derived from this article or parts of it. The images or other third party material in this article are included in the article's Creative Commons licence, unless indicated otherwise in a credit line to the material. If material is not included in the article's Creative Commons licence and your intended use is not permitted by statutory regulation or exceeds the permitted use, you will need to obtain permission directly from the copyright holder. To view a copy of this licence, visit <http://creativecommons.org/licenses/by-nc-nd/4.0/>.

Introduction

Ovarian reserve (OR) reflects the cumulative number of ovarian follicles, which encompasses both non-growing follicles and those in distinct stages of growth, such as antral and preantral stages [1]. Primordial follicles undergo a series of developmental stages, progressing from primary follicles to secondary follicles, and ultimately become mature follicles [2]. OR is a significant predictor of the reproductive capacity of females [3]. Diminished ovarian reserve (DOR) refers to the diminution in reproductive capacity due to diverse factors resulting in a drop in the quantity and quality of ovarian follicles [4, 5]. The predominant clinical presentations of DOR are infertility, menstruation irregularities, endocrine dysfunctions, and poor response to ovarian stimulation; if left untreated, DOR may progress to premature ovarian failure (POF) within a timeframe of 1 to 6 years [6]. Despite the utilization of assisted reproduction as a therapy option, DOR patients experience a notable decrease in pregnancy rates because of their restricted response to ovulation induction medications, and their live birth rate is much lower than that of females with normal OR [7].

Yangjing Zhongyu Decoction (YJZYD), which is documented in classical Chinese medicine, has been employed as a clinically effective remedy for female infertility for centuries, but its effects on ovarian granulosa cells (GCs) need further study [8]. Reportedly, in the H₂O₂-induced human ovarian GC line KGN, YJZYD safeguards ovarian GCs and female fertility by enhancing the synthesis of estrogen, improving energy metabolism, and increasing mitochondrial activity [8]. Besides, YJZYD can alleviate ovarian lesions and reproductive endocrine disorders *in vivo* by modulating cell apoptosis, energy metabolism, and hormone synthesis [9]. YJZYD has also been found to enhance the expression levels of follicle-stimulating hormone receptor (FSHR), IGF-1, and StAR in the ovary, hence ameliorating follicular function and boosting follicle development [10].

Mitochondrial dynamics describes the dynamic behaviors of mitochondria, including mitochondrial mitophagy, fusion, migration, and fission, with mitochondria undergoing continuous alterations in their shape, quantity, and position in response to changes in the intracellular milieu [11]. Specifically, mitochondrial fission and fusion are prerequisites for other mitochondrial regulatory mechanisms [12]. Administering dehydroepiandrosterone offers significant advantages for the outcomes of *in vitro* fertilization in patients with poor ovarian responder (POR), and this beneficial impact may be partially facilitated by the improvement of mitochondrial dynamics in cumulus cells [13]. Therefore, we predicted that YJZYD might regulate mitochondrial dynamics to improve ovarian reserve function decline. Notably, the

process of mitochondrial fission necessitates the presence of dynamin-related protein 1 (Drp1) [14]. As previously reported, the decreased level of the mitochondrial fusion protein mitofusin 2 (MFN2) accelerates GC apoptosis [15]. Also, the loss of the mitochondrial fusion protein MFN1 in oocytes induces alterations in mitochondrial dynamics, which arouse apoptosis and accelerate ovarian follicular reserve failure [16]. Nevertheless, it has not been reported that YJZYD regulates mitochondrial dynamics of ovarian granulosa cells to improve the decline of ovarian reserve function. Furthermore, the mitogen-activated protein kinase (MAPK) and extracellular signal-regulated kinase (ERK) pathways are momentous in the modulation of distinct biological processes involving cell growth, inflammation, differentiation, and apoptosis [17, 18]. For instance, the activation of the ERK pathway by kisspeptin redounds ovarian GC proliferation and concurrently attenuates oxidative damage and apoptosis [19]. Orexin-A impedes mouse GC apoptosis and potentiates their proliferation by stimulating the ERK pathway [20]. The activation of the MAPK/ERK signaling by cryptotanshinone reportedly provides protection against PCOS-induced ovarian tissue damage [21]. However, the mechanism of YJZYD regulating mitochondrial dynamics of ovarian GCs via the MAPK/ERK pathway to improve DOR has been poorly reported, and thus we explore this mechanism to provide reference value for the treatment of patients with DOR.

Materials and methods

Ethics statement

The study was authorized by the academic ethics committee of The Second Affiliated Hospital of Hunan University of Chinese Medicine [NO.2023-45]. All procedures were strictly implemented according to the Declaration of Helsinki and the Guide for the Care and Use of Laboratory Animals. Informed consent was obtained from all parents or legal representatives after they were fully informed of the study objectives. All laboratory procedures were used to minimize the pain of mice.

Study subjects

A total of 161 patients with DOR who received treatment at The Second Affiliated Hospital of Hunan University of Chinese Medicine from January 2021 to December 2022 were selected, among which 30 were excluded as per the inclusion and exclusion criteria, 11 were unwilling to participate, 10 withdrew, and 5 had incomplete data. Finally, 105 patients were included as the study subjects.

The inclusion criteria were as follows [22]: (1) age between 18 and 40 years; (2) 0.5 ng/mL < anti-Mullerian hormone (AMH) < 1.1 ng/mL; (3) antral follicle count (AFC) < 7; (4) 10 IU/L < follicle-stimulating hormone (FSH) < 25 IU/L; (5) clinical manifestations of irregular

menstruation, infertility, oligomenorrhea, amenorrhea, sexual dysfunction, dyspareunia and vaginal dryness; (6) DOR treatment with YJZYD.

The exclusion criteria were as below [22, 23]: (1) previous history of unilateral or bilateral oophorectomy; (2) administration of sex hormones including estrogen, progesterone, and gonadotropins within one week before receiving treatment; (3) diagnosis of corpus luteum cyst, residual follicle, or a space-occupying lesion in the ovary, PCOS, or pelvic inflammatory disease; (4) pregnant or receiving hormone replacement therapy, dehydroepiandrosterone, and other treatment methods; (5) with severe respiratory diseases, cardiovascular diseases, liver and kidney diseases, hematopoietic system diseases or mental illness.

Treatment method

All participants avoided the 1st-4th day of the menstrual period and began to take YJZYD from the 5th day of the menstrual cycle for 21 consecutive days. YJZYD is composed of cooked *Rehmannia glutinosa* (30 g), *Angelica sinensis* (15 g), *Paeonia lactiflora* (15 g), and *Cornus officinalis* (15 g). In the specific compatibility, clinical addition and subtraction should be carried out according to the specific symptoms of the patients, and the prescription should be adjusted accordingly. Each dose of the traditional Chinese medicine was added with 500 mL water, decocted (150 mL/time), and administered to the patients three times a day for consecutive 6 months. Of these, cooked *Rehmannia glutinosa*, *Angelica sinensis*, *Paeonia lactiflora*, and *cornus officinalis* were all purchased from TongRenTang (Beijing, China).

Sample and data collection

Before and after treatment, 5 mL fasting elbow vein blood was gathered from the patients on the 2nd to 3rd day of the menstrual cycle, centrifuged at 2000 r/min for 20 min, and stored in a refrigerator at 4 °C. Serum hormone testing was performed on the same day.

Ultrasound measurement

Ovarian volume (OV), AFC, and endometrial thickness (EMT) pre- and post-treatment were evaluated using ultrasound Voluson E6 (GE, Healthcare, Milwaukee, WI, USA). AFC was the sum of follicles observed in both ovaries using ultrasound in the early follicular phase (on days 2–4) of the menstrual cycle. OV and EMT were documented on days 12–21 of the menstrual cycle.

Experimental animals

Female C57BL/6 mice ($n=36$, 25 ± 2 g, 6 weeks old) were purchased from the experimental animal resource platform of the Chinese Academy of Sciences. Mice were reared in a specific pathogen-free standard animal room

and 12-h light/dark cycle at 23 ± 2 °C, with a relative humidity of 50-60% and free access to food and water.

Establishment of DOR mouse models

After one week of continuous vaginal smear examination, all 36 female mice exhibited regular estrous cycles following a 1-week continuous vaginal smear examination. DOR mouse models were established based on a previous study [24]. Briefly, mice were intraperitoneally injected with cyclophosphamide (Cy) (75 mg/kg, 500 μ L; Endoxan, Shionogi & Co., Osaka, Japan) once a week on the first day of weeks 2–5, with the injection of 0.9% normal saline instead of Cy as the control. Following the treatment, vaginal exfoliated cell smears were conducted to observe the estrous cycle [25]. When the model mice exhibited estrous cycle disorder, it was determined that the DOR mouse models were successfully established.

The mice were randomly divided into the following 9 groups: the Control group: without any treatment; the model group (DOR): intraperitoneal injection of Cy (75 mg/kg, 500 μ L) [24]; the Sal group: intraperitoneal injection of an equal amount of 0.9% normal saline solution; the DOR+YJZYD group: intraperitoneal injection of Cy (75 mg/kg, 500 μ L) and gavage of YJZYD solution (10 mL/kg, 3 mg/ μ L) [9]; the DOR+PW group: intraperitoneal injection of Cy (75 mg/kg, 500 μ L) and gavage of purified water (PW) equivalent to YJZYD solution; the DOR+YJZYD+PD98059 group: intraperitoneal injection of Cy (75 mg/kg, 500 μ L) and PD98059 (1 mg/kg; an ERK inhibitor) [26]; and gavage of YJZYD solution (10 mL/kg), the DOR+YJZYD+Vehicle group: intraperitoneal injection of Cy (75 mg/kg, 500 μ L) and Vehicle equivalent to PD98059 [10% dimethyl sulfoxide (DMSO)+90% (20% SBE- β -CD in Saline)], and gavage of YJZYD solution (10 mL/kg); the DOR+TPA group: intraperitoneal injection of 75 mg/kg (500 μ L) of Cy and 150 μ g/kg 12-O-tetradecanoylphorbol-13-acetate (TPA; an ERK activator) [27]; the DOR+Vehicle 2 group: intraperitoneal injection of 75 mg/kg (500 μ L) of Cy and the same amount of Vehicle (94 mg/mL Ethanol) as TPA. Among them, YJZYD solution was concentrated before vacuum freeze-dried into powder, resuspended in 200 μ L pure water at a concentration of 3 mg/ μ L, and stored at 4 °C for subsequent animal and cell experiments. PD98059 (MedChemExpress, Monmouth Junction, NJ, USA) is an inhibitor of the MAPK/ERK pathway. TPA (Aadoq Bioscience, CA, USA) is an activator of the MAPK/ERK pathway. After 5 weeks, all mice were euthanized with 150 mg/kg pentobarbital sodium, with ovarian and serum samples collected.

Ovarian morphology analysis and AFC

Referring to previous research [25], ovarian morphology analysis and AFC were conducted. Simply put, after fixation with 4% paraformaldehyde, dehydration, and paraffin

embedding, the ovaries were cut into Sect. (5 μm) and subjected to hematoxylin and eosin (HE) staining, with the ovarian morphology observed under an optical microscope (Olympus Corporation, Tokyo, Japan), and the follicle number counted, as reported previously [28]. A primitive follicle is characterized by the presence of a central oogonia that is enveloped by a layer of flat follicular cells. Primary follicles are composed of oocytes and a layer of cubic granulosa cells around them. Secondary follicles are composed of oocytes and their surrounding multi-layer cubic follicular cells. A mature follicle is one in which the follicular lumen is large, the ovarian mound is distinct, the follicular endothelial cells are immediately adjacent to the follicular granulosa and separated from the granulosa cells by a basement membrane, and the endothelial cells are polygonal, with clear cytoplasm and rounded nuclei. Follicular atresia is distinguished by the unclear or complete disappearance of the egg cell's structure, shrinkage of the zona pellucida, and collapse of the follicular wall [2].

Terminal deoxynucleotidyl transferase dUTP nick-end labeling (TUNEL) staining and fluorescence double labeling

Ovarian GCs were identified by the FSHR [29]. After xylene dewaxing and gradient ethanol hydration, mouse ovarian tissue sections were stained with the TUNEL apoptosis detection kit (Elabscience Biotechnology, Wuhan, Hubei, China), followed by 3 washes with tris-buffered saline (TBS) for 5 min and an incubation with rabbit anti-FSHR (1:500, GTX64391, GeneTex, Irvine, CA, USA). Later, the sections were rinsed in TBS before 1-h incubation with secondary antibodies (1:200, GTX26721, GeneTex). A fluorescence microscope (Zeiss, Oberkochen, Germany) was employed to observe the percentage of apoptotic positive cells in each field, and the average was calculated.

Enzyme-linked immunosorbent assay (ELISA)

The levels of serum AMH, FSH, luteinizing hormone (LH), and estradiol (E2) were determined as per the instructions of the ELISA kits. The human AMH ELISA kit, human or mouse FSH ELISA kit, human or mouse LH ELISA kit, and human or mouse E2 ELISA kit were all acquired from Xinfan Biological Technology (Shanghai, China), and the mouse AMH ELISA kit was procured from Fusheng Industrial (Shanghai, China).

Cell culture

Human ovarian GCs (KGN) were acquired from Yubo Biological Technology (Shanghai, China) and identified using the short tandem repeat method. KGN cells were cultured in the Dulbecco's modified Eagle's medium/F12 (Gibco, Grand Island, NY, USA) comprising 10% fetal

bovine serum (Gibco) and 1% antibiotic (Gibco) in an incubator at 37 °C containing 5% CO₂, with the medium changed every 2 days. Cells at a confluence of about 80% in P3 generation were selected for the subsequent experiments. Because Cy was inert *in vitro*, we used 4-Hydroperoxy-Cyclophosphamide (4-HC) (8 μm) (Anjiekai Biomedical Science and Technology, Wuhan, Hubei, China) as an *in vitro* intervention. 4-HC is a precursor of Cy in an activated form [24].

KGN cells were divided into the following 8 groups: the KGN group (blank control without any treatment), the KGN+4-HC group [cells treated with 4-HC (8 μm) for 24 h], the KGN+Vehicle 1 group [cells were treated with an equal amount of Vehicle (30 mg/mL in DMSO) to 4-HC for 24 h], the KGN+4-HC+YJZYD group [cells were treated with 4-HC (8 μm) [30] and YJZYD solution (1 mg/mL) [8] for 24 h], the KGN+4-HC+YJZYD+PD98059 group [cells were cultured with 4-HC (8 μm), YJZYD solution (1 mg/mL), and PD98059 (5 μm) [19] for 24 h], the KGN+4-HC+YJZYD+Vehicle group [cells were treated with 4-HC (8 μm), YJZYD solution (1 mg/mL), Vehicle [10% DMSO+90% (20% SBE- β -CD in Saline)] equivalent to PD98059 for 24 h], the KGN+4-HC+TPA group [cells were subjected to treatment with 8 μm 4-HC and 200 nM TPA [31] for 24 h], and the KGN+4-HC+Vehicle 2 group [cells were treated with 8 μm 4-HC and Vehicle equal to TPA for 24 h].

Cell counting kit-8 (CCK-8) assay

KGN cell suspensions (100 μL /well) were seeded onto a 96-well plate in an incubator at 37 °C containing 5% CO₂ for pre-cultivation. Cell proliferative ability was assessed using the CCK-8 kit (Beyotime, Shanghai, China). Cells were added with 20 μL /well of CCK-8 solution and incubated at 37 °C for 1 h. The absorbance of 24 h, 48 h, and 72 h was measured at 450 nm using a microplate reader (Thermo Fisher Scientific, Shanghai, China).

Flow cytometry

Fluorescein isothiocyanate-Annexin V Apoptosis Detection Kit (BD Biosciences, San Diego, CA, USA) was used to evaluate the apoptosis of KGN cells treated for 24 h. Cells were harvested by trypsin detachment and cultured in the presence of AnnexinV/propidium iodide at 20–25 °C for 20 min. Cell apoptosis was analyzed using a flow cytometer (FACScan, BD Biosciences) equipped with Cell Quest 3.0 software.

Western blot

The total protein solution was extracted by lysis in radioimmunoprecipitation assay buffer (Beyotime). The protein concentration was ascertained using the bicinchoninic acid protein assay kit (Beyotime). An equal

amount of protein (50 μ g) onto sodium dodecyl sulfate-polyacrylamide gel electrophoresis (Thermo Fisher Scientific) for the separation of the target protein. The separated protein was then shifted to a polyvinylidene fluoride membrane (Millipore, Burlington, MA, USA). Thereafter, the membrane was interacted with primary antibodies Anti-Bcl-2 (1:1000, ab32124, Abcam, Cambridge, UK), Anti-Bax (1:1000, ab32503, Abcam), Anti-Cleaved-caspase-3 (1:500, ab32042, Abcam), Anti-phospho (p)-Drp1 Ser616 (1:1000, ab314755, Abcam), Anti-Drp1 (1:1000, ab184247, Abcam), Anti-MFN1 (1:1000, ab191853, Abcam), Anti-MFN2 (1:2000, ab205236, Abcam), Anti-ERK1/2 (1:10000, ab184699, Abcam), Anti-p-ERK1/2 (1:1000, ab201015, Abcam) overnight at 4 °C. Subsequently, the membrane was washed before being interacted with horseradish peroxidase-labeled goat-anti-rabbit secondary antibody (IgG, 1:2000, ab205718, Abcam) at room temperature for 1 h, and then detected using enhanced chemiluminescence. Image J software (National Institutes of Health, Bethesda, MD, USA) was applied to perform grayscale analysis on the bands, with GAPDH as the internal reference. Each experiment was repeated thrice.

Mitochondrial staining

MitoTracker Green reagent (Beyotime) was used to determine the number of mitochondria in each group of KGN cell treated for 24 h. After various treatments, cells were washed with 1 \times phosphate-buffered saline (PBS) three times and incubated with MitoTracker Green reagent for 30 min. Finally, after 3 washes with 1 \times PBS, cells were subjected to Hoechst staining for 10 min and imaging under a fluorescence microscope (Zeiss). The mitochondria number was counted using Image J (National Institutes of Health), and the average number of mitochondria in each cell was analyzed.

Table 1 Changes in indicator levels before and after treatment in patients with DOR

Parameters	Before Treatment (n = 105)	After Treatment (n = 105)	P value
AMH (ng/mL)	0.80 \pm 0.09	0.87 \pm 0.15	< 0.0001
FSH (IU/L)	16.91 \pm 2.14	15.36 \pm 2.70	< 0.0001
LH (IU/L)	13.78 \pm 2.06	7.64 \pm 2.40	< 0.0001
E2 (pg/mL)	35.03 \pm 8.02	55.32 \pm 10.11	< 0.0001
OV (cm ³)	3.13 \pm 0.35	4.11 \pm 0.75	< 0.0001
AFC (pcs)	3 (1,4)	3 (1,5)	0.0086
EMT (mm)	6.05 \pm 1.04	7.02 \pm 1.34	< 0.0001

Note AMH: anti-Mullerian hormone; FSH: follicle-stimulating hormone; LH: luteinizing hormone; E2: estradiol; OV: ovarian volume; AFC: antral follicle count; EMT: endometrium thickness. The data that conformed to the normal distribution were represented by the mean \pm standard deviation, and tested between two groups using the paired *t* test. Non-normal distribution data were represented by median values (minimum, maximum), and data comparisons between two groups were conducted using the Wilcoxon matched-pairs signed rank test

Statistical analysis

All data were statistically analyzed and plotted using GraphPad Prism 8.01 (GraphPad Software, San Diego, CA, USA). The Shapiro-Wilk test method was used to test the normal distribution. The measurement data of the normal distribution were expressed as mean \pm standard deviation (SD), and the paired *t* test was used for inter-group comparisons. Non-normal distribution measurement data were expressed in quartiles, and inter-group comparisons were conducted using the Wilcoxon matched-pairs signed rank test. One-way analysis of variance (ANOVA) was adopted for multi-inter group comparisons, and Tukey's multiple comparisons test was utilized for post hoc testing. The difference was statistically significant with *P* < 0.05.

Results

YJZYD improved DOR

The changes in indicator levels before and after treatment were compared among all subjects. As shown in Table 1, AMH, E2, OV, AFC, and EMT were saliently increased in DOR patients after treatment, while FSH and LH levels were decreased (all *P* < 0.05).

YJZYD improved ovarian function in DOR mice

To investigate the effect of YJZYD on ovarian function in DOR mice, female mice that showed regular estrous cycles in 1-week continuous vaginal smear examination were intraperitoneally injected with Cy on the first day of weeks 2–5, in a bid to establish a DOR mouse model for in vivo experiments. As shown in Fig. 1A, mice were subjected to random grouping, and we initially compared the estrous cycles of the Sal group and the DOR group after Cy induction. In the Sal group, all mice had regular estrous cycles, while in the DOR group, all mice exhibited irregular estrous cycles subsequent to Cy induction (Fig. 1B). Compared with the Sal group, the DOR group had saliently diminished levels of serum AMH and E2 and obviously raised levels of FSH and LH (all *P* < 0.001) (Fig. 1C–F). In comparison with the Sal group, the number of follicles in each stage (primitive follicles, primary follicles, secondary follicles, and mature follicles) in the DOR group was evidently reduced, and the number of atresia follicles in the DOR group was apparently increased (all *P* < 0.001), along with the disordered arrangement of GCs and more severe interstitial fibrosis (Fig. 1G–H). Moreover, the number of TUNEL staining-positive GCs in DOR mice was prominently higher than that of the Sal group (*P* < 0.01) (Fig. 1I). Furthermore, we treated DOR mice with 10 mL/kg of YJZYD solution, with the results manifesting apparent decreases in the proportion of irregular estrous cycles, serum FSH and LH levels, the number of atresia follicles, and GC apoptosis, as well as obvious increases in levels of serum

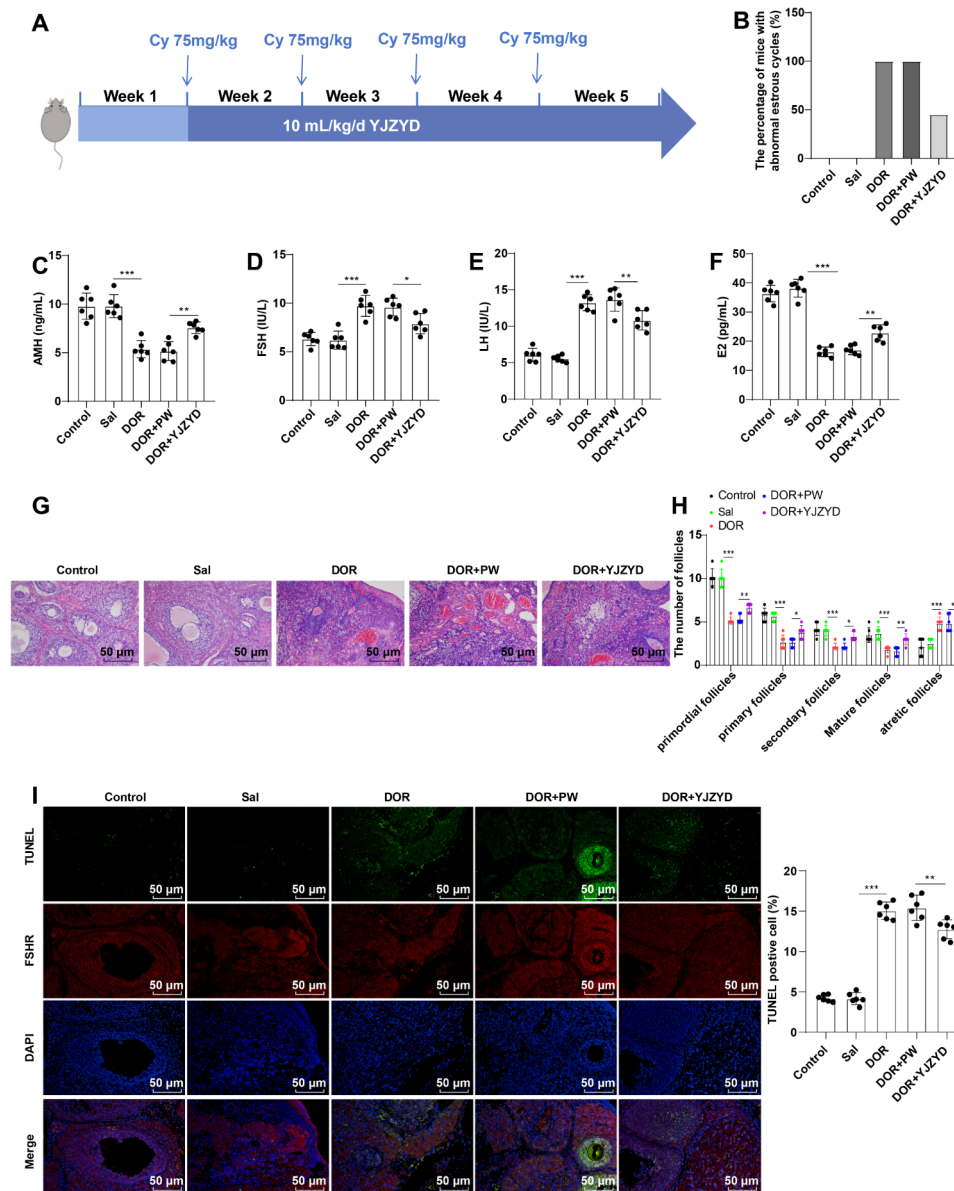


Fig. 1 YJZYD improved ovarian function in DOR mice. **A:** In vivo experimental protocol in mice; **B:** Vaginal smear detection for estrus cycle; **C-F:** ELISA detection of serum AMH, FSH, LH, and E2 levels; **G-H:** HE staining to observe the morphology of the ovaries and compare changes in the number of follicles; **I:** TUNEL staining and FSHR co-labeling to assess apoptosis of ovarian GCs in ovarian tissues. $n=6$. Data were expressed as mean \pm SD. Multiple-group comparisons were statistically analyzed using one-way ANOVA, and post hoc tests were conducted using Tukey's multiple comparison test. * $P < 0.05$, ** $P < 0.01$, *** $P < 0.001$

AMH and E2 and the number of follicles at each stage (all $P < 0.05$) (Fig. 1B-I). These results suggested that YJZYD improved the ovarian function in DOR mice.

YJZYD promoted the proliferation of human ovarian GCs (KGN) treated with 4-HC and inhibited their apoptosis

To examine the impacts of YJZYD on the proliferation and apoptosis of KGN cells, we first treated KGN with 4-HC and assessed cell proliferation using the CCK-8 assay. The KGN+4-HC group showed an evident abatement in cell proliferation in comparison to

the KGN+Vehicle 1 group ($P < 0.001$) (Fig. 2A). Also, there was a substantially higher apoptotic rate in the KGN+4-HC group than in the KGN+Vehicle 1 group ($P < 0.001$) (Fig. 2B). Besides, as shown by Western blot, the expression levels of Bax and Cleaved-caspase-3 rose, while Bcl-2 expression dropped in the KGN+4-HC group versus the KGN+Vehicle 1 group (all $P < 0.001$) (Fig. 2C). Subsequently, after simultaneously being treated with 4-HC and YJZYD solution, KGN cells exhibited memorably augmented cell proliferative ability, limited cell apoptosis, suppressed expression levels of Bax

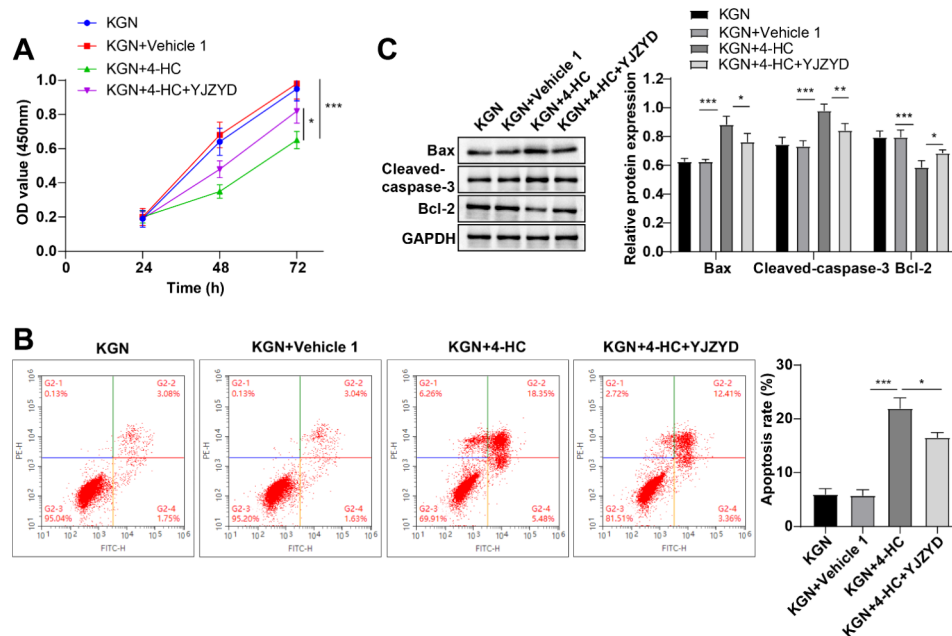


Fig. 2 YJZYD facilitated the proliferation of 4-HC-treated KGN and inhibited cell apoptosis. **A:** CCK-8 detection of cell proliferation; **B:** Flow cytometry analysis of cell apoptosis. The X-axis and Y-axis values in the flow chart refer to the fluorescence intensity of Annexin V and PI. The flow diagram was divided into four quadrants, with upper left quadrant Q1 (Annexin⁻/PI⁺) representing mechanically damaged cells, upper right quadrant Q2 (Annexin⁺/PI⁺) denoting late apoptotic cells, lower right quadrant Q3 (Annexin⁺/PI⁻) representing early apoptotic cells, and lower left quadrant Q4 (Annexin⁻/PI⁻) indicating normal/viable cells. The apoptotic rate was the sum of the percentage of Q2 and Q3 quadrants; **C:** Western blot to determine the expression levels of apoptosis-related proteins (Bax, Cleaved-caspase-3, and Bcl-2). Data were expressed as mean \pm SD. Multiple-group comparisons were statistically analyzed using one-way ANOVA, and post hoc tests were conducted using Tukey's multiple comparison test. * $P < 0.05$, ** $P < 0.01$, *** $P < 0.001$

and Cleaved-caspase-3, and potentiated Bcl-2 expression in the KGN+4-HC+YJZYD group relative to the KGN+4-HC group (all $P < 0.05$) (Fig. 2A-C). The above results suggested that YJZYD stimulated 4-HC-treated KGN cell proliferation and repressed their apoptosis.

YJZYD suppressed mitochondrial fission and promoted mitochondrial fusion in 4-HC-treated KGN cells

Firstly, we detected mitochondrial fragments by Mito-Tracker staining and counted the number of mitochondria. In contrast to the KGN+Vehicle 1 group, the KGN+4-HC group showed augmented mitochondrial fission and its quantity, whereas after treating with both 4-HC and YJZYD solution, cells exhibited reduced mitochondrial fission and quantity (all $P < 0.05$) (Fig. 3A-B). Drp1 is an essential core molecule for controlling mitochondrial cleavage, and phosphorylation at the serine 616 site of Drp1 can promote Drp1 activity, thereby promoting cell division [32]. Subsequently, the protein expression levels of mitochondrial fission-related proteins (Drp1, p-Drp1 Ser616) and mitochondrial fusion-related proteins (MFN1, MFN2) were determined by Western blot. The expression of p-Drp1 (Ser616) protein was remarkably up-regulated, while the expression patterns of MFN1 and MFN2 proteins were prominently down-regulated in the KGN+4-HC group versus the KGN+Vehicle 1 group (all $P < 0.001$) (Fig. 3C); however, after 4-HC and YJZYD

solution treatment, the p-Drp1 (ser616) protein expression was apparently diminished, while the expression levels of MFN1 and MFN2 proteins were evidently elevated (all $P < 0.05$) (Fig. 3C). Besides, no apparent change was found in the protein expression of Drp1 in each group (all $P > 0.05$) (Fig. 3C). Altogether, these results indicated that YJZYD suppressed mitochondrial fission and facilitated mitochondrial fusion in 4-HC-treated KGN cells.

YJZYD regulated mitochondrial dynamics, proliferation, and apoptosis in 4-HC-treated KGN cells by activating the MAPK/ERK pathway

Firstly, Western blot detection showed that compared with the KGN+Vehicle 1 group, the levels of p-ERK1/2/ERK1/2 in the KGN+4-HC group were obviously reduced, and the levels in the KGN+4-HC+YJZYD group were noticeably higher than those in the KGN+4-HC group (all $P < 0.01$) (Fig. 4A). Thereafter, while treating KGN with 4-HC or YJZYD solution, we added the MAPK/ERK pathway inhibitor (PD98059). The results delineated that in contrast to the KGN+4-HC+YJZYD+Vehicle group, in the KGN+4-HC+YJZYD+PD98059 group, the levels of p-ERK1/2/ERK1/2 were diminished, the cell proliferative ability was weakened, the apoptotic rate was enhanced, the expression levels of Bax and Cleaved-caspase-3 rose, the expression of Bcl-2 was abated, mitochondrial fission

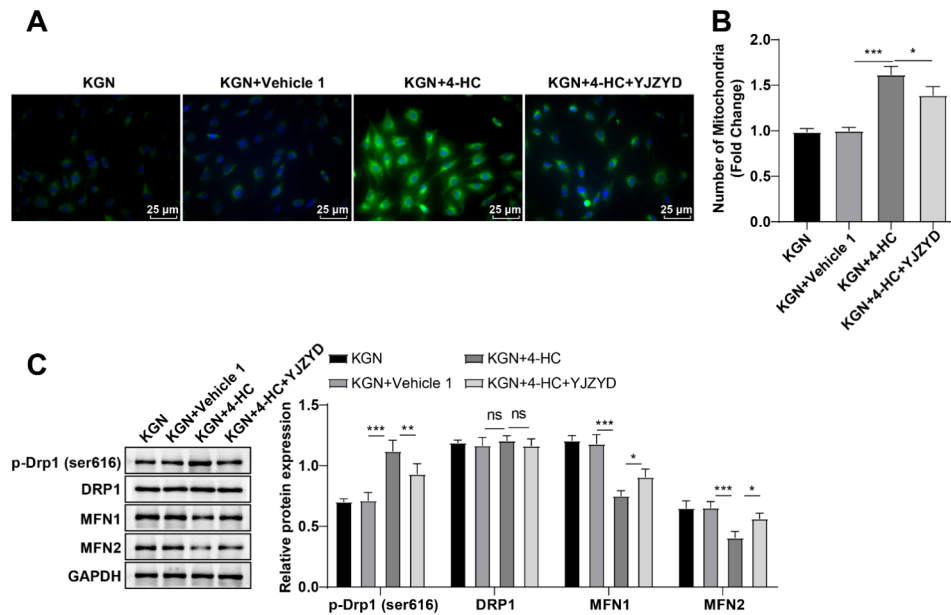


Fig. 3 YJZYD suppressed mitochondrial fission and stimulated mitochondrial fusion in 4-HC-treated KGN cells. **A-B:** MitoTracker staining to detect the number of mitochondrial fragments and count the number of mitochondria; **C:** Western blot to measure protein expression levels of mitochondrial fission-related proteins (Drp1, p-Drp1 Ser616) and mitochondrial fusion-related proteins (MFN1, MFN2). Data were expressed as mean \pm SD. Multiple-group comparisons were statistically analyzed using one-way ANOVA, and post hoc tests were conducted using Tukey's multiple comparison test. ns represented $P > 0.05$, * $P < 0.05$, ** $P < 0.01$, *** $P < 0.001$

and quantity were increased, the expression of p-Drp1 (Ser616) protein was apparently elevated, and the expression patterns of MFN1 and MFN2 proteins were prominently lessened (all $P < 0.05$) (Fig. 4A-G). Additionally, we treated KGN cells with 4-HC and added the MAPK/ERK pathway activator TPA simultaneously. Compared with the KGN+4-HC+Vehicle 2 group, the level of p-ERK1/2/ERK1/2 in the KGN+4-HC+TPA group was observably augmented, which promoted cell proliferation and mitochondrial fusion, and repressed cell apoptosis and mitochondrial fission ($P > 0.05$) (Fig. 4A-G). The above results suggested that YJZYD modulated mitochondrial dynamics, apoptosis, and proliferation in 4-HC-treated KGN cells by activating the MAPK/ERK pathway.

YJZYD improved ovarian function in DOR mice by activating the MAPK/ERK pathway

Finally, for in vivo animal experiment validation, we measured the expression levels of ERK1/2 and p-ERK1/2 in ovarian tissue homogenate using Western blot. Compared with the Control group, p-ERK1/2/ERK1/2 levels were prominently diminished in the DOR group, and the levels in the ovarian tissue homogenate of the DOR+YJZYD group were substantially higher than those of the DOR+PW group (all $P < 0.001$) (Fig. 5A). Subsequently, we intraperitoneally injected mice with Cy, 1 mg/kg of PD98059, and gavaged them with YJZYD solution. Compared to the DOR+YJZYD+Vehicle group, the DOR+YJZYD+PD98059 group showed substantially

down-regulated p-ERK1/2/ERK1/2 levels, increased irregular estrous cycle proportions, decreased serum AMH and E2 levels, and augmented FSH and LH levels in DOR mice; besides, the number of follicles at each stage was conspicuously reduced, the number of atresia follicles was significantly uplifted, GCs were disordered, and GC apoptosis was dramatically promoted (all $P < 0.05$) (Fig. 5A-I). Additionally, we treated mice with intraperitoneal injection of Cy and 150 μ g/kg TPA. Compared to the DOR+Vehicle 2 group, the p-ERK1/2/ERK1/2 level in the DOR+TPA group notably rose, which effectively improved the decline of ovarian reserve function in DOR mice (all $P < 0.001$) (Fig. 5A-I). These results implied that YJZYD ameliorated ovarian function in DOR mice by activating the MAPK/ERK pathway.

Discussion

OR is responsible for determining the length of a woman's reproductive lifespan, which can last several decades due to the robust preservation of meiotic arrest in oocytes located in primordial follicles [33]. The fertility of women with DOR has decreased, whereas the precise mechanisms governing ovarian function in this population have not been fully understood [34]. Encouragingly, YJZYD is a therapeutically utilized treatment for a wide variety of diseases associated with infertility, PCOS, endometrial thinness, implant failure, and premature ovarian insufficiency-related conditions [35]. By conducting animal

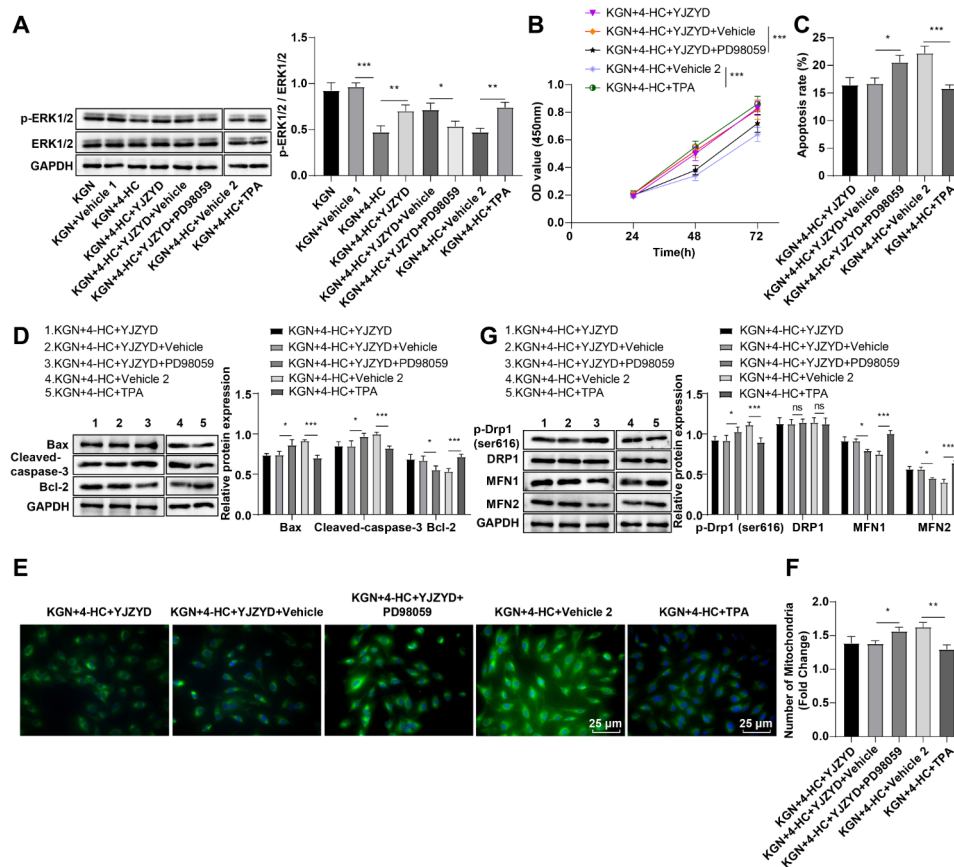


Fig. 4 YJZYD regulated mitochondrial dynamics, proliferation, and apoptosis in 4-HC-treated KGN cells by activating the MAPK/ERK pathway. **A**: Western blot to measure the expression levels of ERK1/2 and p-ERK1/2 in KGN cells; **B**: CCK-8 detection of cell proliferation; **C**: Flow cytometry analysis of cell apoptosis; **D**: Western blot to assess the expression levels of apoptosis-related proteins (Bcl-2, Bax, and Cleaved-caspase-3); **E**: MitoTracker staining to detect the number of mitochondrial fragments and count the number of mitochondria; **F**: MitoTracker staining to detect the number of mitochondrial fragments and count the number of mitochondria; **G**: Western blot to test protein expression patterns of mitochondrial fission-related proteins (Drp1, p-Drp1 Ser616) and mitochondrial fusion-related proteins (MFN1, MFN2). Data were expressed as mean \pm SD. Multiple-group comparisons were statistically analyzed using one-way ANOVA, and post hoc tests were conducted using Tukey's multiple comparison test. ns represented $P > 0.05$, * $P < 0.05$, ** $P < 0.01$, *** $P < 0.001$

and clinical experiments, the present study revealed that YJZYD could effectively improve DOR.

Chinese medicinal herbs are useful in managing DOR by controlling levels of gonadotropin-releasing hormone and ovarian sex hormones, which in turn trigger ovulation [36]. More specifically, the combination of *Semen Cuscutae chinensis*, *Rehmannia glutinosa*, *Fructus mori*, *Radix Morindae officinalis*, and *Fructus lycii* is frequently observed in the treatment of infertility attributed to ovarian factors, including primary ovarian insufficiency, POE, and PCOS [37–39]. Notably, YJZYD comprises four traditional Chinese medicines, namely cooked *Rehmannia glutinosa*, *Angelica sinensis*, *Cornus officinalis*, and *Paeonia lactiflora*, possessing various advantageous properties with regard to blood and kidney nourishment, essence replenishment, and flush modulation [40]. Generally, the higher-than-normal level of FSH often suggests the existence of ovarian abnormalities, like POF [41]. In our clinical trial, after YJZYD treatment, ODR patients exhibited

elevated levels of E2, AMH, OV, AFC, and EMT and reduced levels of LH and FSH. As expected, in a DOR mouse model, we also observed augmented AMH/E2 levels and follicle number and lessened FSH/LH levels, irregular estrus cycle proportions, atresia follicle number, and GC apoptosis after YJZYD treatment. Supporting this viewpoint, it has been reported that Kuntai capsules containing cooked *Rehmannia glutinosa* exert regulatory effects on endometrial receptivity and the human body's response to gonadotropin [42]. Meanwhile, evidence shows that YJZYD encourages EMT, ameliorates endometrial receptivity, and raises clinical pregnancy rates [40]. These results might provide novel evidence for YJZYD to ameliorate DOR, whether in humans or mice.

Reportedly, YJZYD can alleviate reproductive endocrine disorders and ovarian lesions in the body by regulating mechanisms like hormone production and cell apoptosis [9]. 4-HC is an artificially produced substance that undergoes spontaneous conversion to active

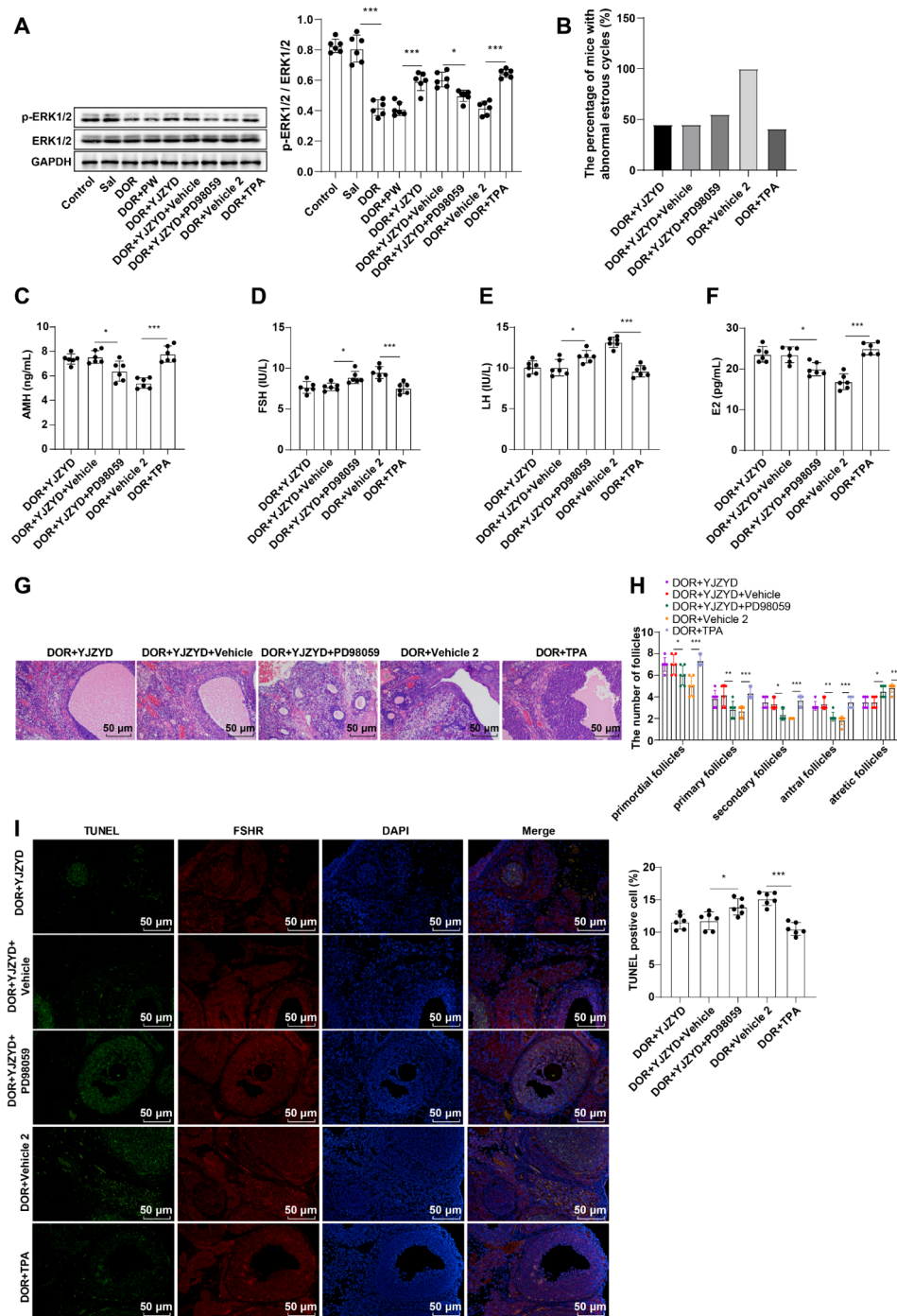


Fig. 5 YJZYD improved ovarian function in DOR mice by activating the MAPK/ERK pathway. **A**: Western blot to determine the expression patterns of ERK1/2 and p-ERK1/2 in mouse ovarian tissue homogenate; **B**: Vaginal smear detection for estrus cycle; **C-F**: ELISA detection of serum AMH, FSH, LH and E2 levels; **G-H**: HE staining to observe the morphology of the ovaries and compare changes in the number of follicles; **I**: TUNEL staining and FSHR co-labeling to evaluate apoptosis of ovarian GCs in ovarian tissues. $n=6$. Data were expressed as mean \pm SD. Multiple-group comparisons were statistically analyzed using one-way ANOVA, and post hoc tests were conducted using Tukey's multiple comparison test. * $P < 0.05$, ** $P < 0.01$, *** $P < 0.001$

metabolites when dissolved in water [43]. Prior research has documented a dramatic drop in primordial follicle count following the administration of 4-HC to the ovary [44]. Additionally, the administration of 4-HC resulted in the initiation of apoptotic cell death, specifically in

mouse dermal endothelial cells [45]. Consistent with these reports, our findings also discovered impeded KGN proliferation and Bcl-2 levels, and elevated apoptotic rate and levels of Bax and Cleaved-caspase-3 following 4-HC treatment. Interestingly, the further treatment of YJZYD

could reverse these trends. Similarly, primary cultures of mouse fibroblasts lead to a dose-dependent rise in cell proliferation after *paoniflorin* treatment [46]. Another study revealed that *Angelica sinensis* suppresses apoptosis and inflammation in an *in vivo* model of spinal cord injury [47]. In addition, morroniside isolated from *Cornus officinalis* has been shown to stimulate cell growth and differentiation, control lipid synthesis, lessen inflammatory responses, and protect against apoptosis [48–51]. Taken together, YJZYD limited apoptosis and stimulated proliferation in human ovarian GCs treated with 4-HC.

The importance of mitochondrial fusion and fission processes in preserving cellular homeostasis has been thoroughly demonstrated in diverse cell types, including fibroblasts, neurons, and epithelial cells [52–54]. MFN1 and MFN2 are found to intensify fusion in the outer mitochondrial membrane [55], whereas the protein p-Drp1 (ser616) plays a vital role in potentiating Drp1-mediated mitochondrial fission and guaranteeing the preservation of cellular homeostasis [56]. Noteworthy, we observed the obviously reduced p-Drp1 protein level and raised MFN1/MFN2 protein levels after treatment with YJZYD in KGN cells. Similar effects have been observed in other studies. For example, the facilitated expression of Drp1 has been confirmed in rats with middle cerebral artery occlusion and is abolished by the administration of a combination of *Panax ginseng* and *Angelica sinensis*, which partly attenuates cerebral injury by improving Drp1-mediated mitochondrial fission [57]. Conjointly, this study discovered for the first time that YJZYD prevented mitochondrial fission and boosted mitochondrial fusion in KGN cells treated with 4-HC.

The ERK/MAPK pathway accelerates cellular proliferation and offers a protective effect against apoptosis [58]. Of note, our findings revealed that the treatments of 4-HC or YJZYD, and PD98059 brought about decreased p-ERK1/2/ERK1/2 level, cell proliferation, Bcl-2 expression and MFN1/MFN2 protein levels, and increased cell apoptotic rate, Bax/Cleaved-caspase-3 levels, mitochondrial fission and number, and p-Drp1 expression in KGN cells; conversely, TPA treatment on KGN cells upon 4-HC treatment brought about increased p-ERK1/2/ERK1/2 level, facilitating mitochondrial fusion and cell proliferation, and limiting mitochondrial fission and cell apoptosis. In line with our findings, the application of PD98059, an inhibitor of MAPK/ERK kinase, resulted in the inhibition of ERK activation generated by ischemia/reperfusion and an elevation in the number of apoptotic cells in myocytes [59]. The suppressive effects of T-box transcription factor 21 on mitochondrial fission and cell death were partly annulled by curbing the MAPK/ERK pathway [60]. Specifically, Haiyan Jia et al. have reported that the primary mechanism by which human leukemic cells proliferate is through the stimulation of the

MAPK/ERK pathway [61]. Additionally, the activation of the MEK/ERK cascade can weaken the ability of VEGF to shield neurons from apoptosis caused by mechanical trauma [62]. Thus, it could be plausible that YJZYD modulated the mitochondrial dynamics, proliferation, and apoptosis in KGN cells by activating the MAPK/ERK pathway. Meanwhile, the treatments of YJZYD and PD98059 also led to reduced p-ERK1/2/ERK1/2 level, serum AMH and E2 levels and the number of follicles at each stage, and increased proportion of irregular estrous cycles, FSH and LH levels, the number of atresia follicles, and GC apoptosis in mouse ovarian tissues, while TPA treatment elevated p-ERK1/2/ERK1/2 level, effectively improving the decline of ovarian reserve function in DOR mice. Collectively, these data suggested that YJZYD ameliorated DOR in mice via activation of the MAPK/ERK pathway.

In conclusion, by culturing human ovarian GC KGN cells in ODR mice and clinically including DOR patients as study subjects, the current study underlined that YJZYD promoted the proliferation and mitochondrial fusion of ovarian GC cells, inhibited apoptosis and mitochondrial fission, and effectively ameliorated DOR in mice and patients through activating the MAPK/ERK pathway. However, this study only explored the effects of YJZYD on mitochondrial fission and fusion, with the molecular mechanism of YJZYD largely unknown, which needed to be studied more comprehensively and deeply.

Acknowledgements

Not applicable.

Author contributions

All authors contributed to the study conception and design, and all authors commented on previous versions of the manuscript. All authors read and approved the final manuscript. All persons designated as authors qualify for authorship, and all those who qualify for authorship are listed. P.L. was responsible for the integrity assurance of the entire research, the definition of knowledge content and literature research, experimental research, data analysis, manuscript preparation and manuscript editing. J.K. was responsible for ensuring the integrity of the entire research and the definition of the knowledge content. She has contributed to literature research, experimental research, manuscript preparation, manuscript editing and statistical analysis.

Funding

Not applicable.

Data availability

The data that support the findings of this study are available from the corresponding author upon reasonable request.

Declarations

Ethical approval

The study was authorized by the academic ethics committee of The Second Affiliated Hospital of Hunan University of Chinese Medicine (NO.2023-45). All procedures were strictly implemented according to the Declaration of Helsinki and the Guide for the Care and Use of Laboratory Animals. Informed consent was obtained from all parents or legal representatives after they were fully informed of the study objectives. All laboratory procedures were used to minimize the pain of mice.

Submission declaration and verification

The work described has not been published previously, that it is not under consideration for publication elsewhere, that its publication is approved by all authors and tacitly or explicitly by the responsible authorities where the work was carried out, and that, if accepted, it will not be published elsewhere in the same form, in English or in any other language, including electronically without the written consent of the copyright-holder.

Consent for publication

Not applicable.

Competing interests

The authors declare no competing interests.

Received: 3 January 2024 / Accepted: 26 August 2024

Published online: 17 September 2024

References

- Fabregues F, Ferreri J, Mendez M, Calafell JM, Otero J, Farre R. In Vitro Follicular activation and stem cell therapy as a Novel treatment strategies in diminished Ovarian Reserve and primary ovarian insufficiency. *Front Endocrinol (Lausanne)*. 2020;11:617704.
- Myers M, Britt KL, Wreford NG, Ebling FJ, Kerr JB. Methods for quantifying follicular numbers within the mouse ovary. *Reproduction*. 2004;127(5):569–80.
- Li J, Zhang Z, Wei Y, Zhu P, Yin T, Wan Q. Metabonomic analysis of follicular fluid in patients with diminished ovarian reserve. *Front Endocrinol (Lausanne)*. 2023;14:1132621.
- Wan Y, Hong Z, Ma B, He X, Ma L, Wang M, et al. Identification of compound heterozygous variants in MSH4 as a novel genetic cause of diminished ovarian reserve. *Reprod Biol Endocrinol*. 2023;21(1):76.
- Wang J, Pan X, Zhou J, Li X, Sun Y, Wang L. Advances in understanding the effect and mechanism of dehydroepiandrosterone on diminished ovarian reserve. *Drug Discov Ther*. 2023;17(2):87–94.
- Liang C, Zhang X, Qi C, Hu H, Zhang Q, Zhu X, et al. UHPLC-MS-MS analysis of oxylipins metabolomics components of follicular fluid in infertile individuals with diminished ovarian reserve. *Reprod Biol Endocrinol*. 2021;19(1):143.
- Hu S, Xu B, Jin L. Perinatal outcome in young patients with diminished ovarian reserve undergoing assisted reproductive technology. *Fertil Steril*. 2020;114(1):118–24. e1.
- Liu J, Shi D, Ma Q, Zhao P. Yangjing Zhongyu decoction facilitates mitochondrial activity, estrogenesis, and energy metabolism in H(2)O(2)-induced human granulosa cell line KGN. *J Ethnopharmacol*. 2022;295:115398.
- Liu J, Wei B, Ma Q, Shi D, Pan X, Liu Z, et al. Network pharmacology and experimental validation on yangjing zhongyu decoction against diminished ovarian reserve. *J Ethnopharmacol*. 2024;318:117023. Pt B).
- Ma HX, Xie J, Lai MH. [Effects of Yangling Zhongyu Decoction on the secretion of ovarian granule cells in polycystic ovarian syndrome rat model]. *Zhongguo Zhong Xi Yi Jie He Za Zhi*. 2012;32(1):54–7.
- Hao Y, Zhao L, Zhao JY, Han X, Zhou X. Unveiling the potential of mitochondrial dynamics as a therapeutic strategy for acute kidney injury. *Front Cell Dev Biol*. 2023;11:1244313.
- Chan DC. Mitochondrial dynamics and its involvement in Disease. *Annu Rev Pathol*. 2020;15:235–59.
- Hou YL, Li CJ, Lin LT, Chen SN, Wen ZH, Tsui KH. DHEA restores mitochondrial dynamics of cumulus cells by regulating PGAM5 expression in poor ovarian responders. *Taiwan J Obstet Gynecol*. 2022;61(2):223–9.
- Osellame LD, Singh AP, Stroud DA, Palmer CS, Stojanovski D, Ramachandran R, et al. Cooperative and independent roles of the Drp1 adaptors Mff, MiD49 and MiD51 in mitochondrial fission. *J Cell Sci*. 2016;129(11):2170–81.
- Wang L, Song S, Liu X, Zhang M, Xiang W. Low MFN2 expression related to ageing in granulosa cells is associated with assisted reproductive technology outcome. *Reprod Biomed Online*. 2019;38(2):152–8.
- Zhang M, Bener MB, Jiang Z, Wang T, Esencan E, Scott Iii R, et al. Mitofusin 1 is required for female fertility and to maintain ovarian follicular reserve. *Cell Death Dis*. 2019;10(8):560.
- Shen M, Li T, Feng Y, Wu P, Serrano BR, Barcenar AR, et al. Effects of quercetin on granulosa cells from prehierarchal follicles by modulating MAPK signaling pathway in chicken. *Poult Sci*. 2023;102(7):102736.
- Sheppard KE, Cullinane C, Hannan KM, Wall M, Chan J, Barber F, et al. Synergistic inhibition of ovarian cancer cell growth by combining selective PI3K/mTOR and RAS/ERK pathway inhibitors. *Eur J Cancer*. 2013;49(18):3936–44.
- Sun P, Zhang Y, Sun L, Sun N, Wang J, Ma H. Kisspeptin regulates the proliferation and apoptosis of ovary granulosa cells in polycystic ovary syndrome by modulating the PI3K/AKT/ERK signalling pathway. *BMC Womens Health*. 2023;23(1):15.
- Safdar M, Liang A, Rajput SA, Abbas N, Zubair M, Shaukat A et al. Orexin-A regulates follicular growth, proliferation, cell cycle and apoptosis in mouse primary granulosa cells via the AKT/ERK signaling pathway. *Molecules*. 2021;26(18).
- Liu H, Xie J, Fan L, Xia Y, Peng X, Zhou J, et al. Cryptotanshinone protects against PCOS-Induced damage of ovarian tissue via regulating oxidative stress, mitochondrial membrane potential, inflammation, and apoptosis via regulating ferroptosis. *Oxid Med Cell Longev*. 2022;2022:8011850.
- Xu Z, Ruan X, Xu X, Yang Y, Cheng J, Luo S, et al. Efficacy and safety of Zi Gui Nu Zhen(RR) capsules used in TCM for fertility preservation in patients with diminished ovarian reserve. *Gynecol Endocrinol*. 2022;38(1):73–7.
- Zhou J, Pan XY, Lin J, Zhou Q, Lan LK, Zhu J, et al. Effects of Bushen Yiqi Huoxue Decoction in treatment of patients with diminished Ovarian Reserve: a Randomized Controlled Trial. *Chin J Integr Med*. 2022;28(3):195–201.
- Zhu F, Gao J, Zeng F, Lai Y, Ruan X, Deng G. Hyperoside protects against cyclophosphamide induced ovarian damage and reduced fertility by suppressing HIF-1alpha/BNIP3-mediated autophagy. *Biomed Pharmacother*. 2022;156:113743.
- Ling L, Feng X, Wei T, Wang Y, Wang Y, Wang Z, et al. Human amnion-derived mesenchymal stem cell (hAD-MSC) transplantation improves ovarian function in rats with premature ovarian insufficiency (POI) at least partly through a paracrine mechanism. *Stem Cell Res Ther*. 2019;10(1):46.
- Qi JY, Yu J, Huang DH, Guo LH, Wang L, Huang X, et al. Salvianolate reduces murine myocardial ischemia and reperfusion injury via ERK1/2 signaling pathways in vivo. *Chin J Integr Med*. 2017;23(1):40–7.
- Choban PS, McKnight T, Flancbaum L, Sabourin CL, Bijur GN, Boros LG, et al. Characterization of a murine model of acute lung injury (ALI): a prominent role for interleukin-1. *J Invest Surg*. 1996;9(2):95–109.
- Wang Z, Wang Y, Yang T, Li J, Yang X. Study of the reparative effects of menstrual-derived stem cells on premature ovarian failure in mice. *Stem Cell Res Ther*. 2017;8(1):11.
- Zhang J, Yin H, Jiang H, Du X, Yang Z. The protective effects of human umbilical cord mesenchymal stem cell-derived extracellular vesicles on cisplatin-damaged granulosa cells. *Taiwan J Obstet Gynecol*. 2020;59(4):527–33.
- Ghosal MK, Ray AK. Assessment of Psychiatric disorders in Consultation-Liaison setting. *Indian J Psychiatry*. 2022;64(Suppl 2):S211–27.
- Meng Y, Qiu SQ, Wang Q, Zuo JL. Regulator of G protein signalling 18 promotes osteocyte proliferation by activating the extracellular signal-regulated kinase signalling pathway. *Int J Mol Med*. 2024;53(3).
- Kraus F, Roy K, Pucadyil TJ, Ryan MT. Function and regulation of the divisome for mitochondrial fission. *Nature*. 2021;590(7844):57–66.
- Hu M, Yeh YH, Munakata Y, Abe H, Sakashita A, Maezawa S, et al. PRC1-mediated epigenetic programming is required to generate the ovarian reserve. *Nat Commun*. 2022;13(1):4510.
- Li H, Wang X, Mu H, Mei Q, Liu Y, Min Z, et al. Mir-484 contributes to diminished ovarian reserve by regulating granulosa cell function via YAP1-mediated mitochondrial function and apoptosis. *Int J Biol Sci*. 2022;18(3):1008–21.
- Lin J, Ma H, Li H, Han J, Guo T, Qin Z, et al. The treatment of complementary and alternative medicine on female infertility caused by endometrial factors. *Evid Based Complement Alternat Med*. 2022;2022:4624311.
- Zhang C, Xu X. Advancement in the treatment of diminished ovarian reserve by traditional Chinese and western medicine. *Exp Ther Med*. 2016;11(4):1173–6.
- Chao SL, Huang LW, Yen HR. Pregnancy in premature ovarian failure after therapy using Chinese herbal medicine. *Chang Gung Med J*. 2003;26(6):449–52.
- Hu Q, Noor M, Wong YF, Hylands PJ, Simmonds MS, Xu Q, et al. In vitro anti-fibrotic activities of herbal compounds and herbs. *Nephrol Dial Transpl*. 2009;24(10):3033–41.
- Hung YC, Kao CW, Lin CC, Liao YN, Wu BY, Hung IL, et al. Chinese Herbal Products for Female Infertility in Taiwan: a Population-based Cohort Study. *Med (Baltim)*. 2016;95(11):e3075.
- Zhang L, Li H, Zhang L, Zu Z, Xu D, Zhang J. Network Pharmacology Analysis of the mechanisms underlying the Therapeutic effects of Yangjing Zhongyu Tang on Thin Endometrium. *Drug Des Devel Ther*. 2023;17:1805–18.

41. Saadia Z. Follicle stimulating hormone (LH: FSH) ratio in polycystic ovary syndrome (PCOS) - obese vs. non- obese women. *Med Arch*. 2020;74(4):289–93.
42. Lin XM, Chen M, Wang QL, Ye XM, Chen HF. Clinical observation of Kuntai capsule combined with Fenmotong in treatment of decline of ovarian reserve function. *World J Clin Cases*. 2021;9(28):8349–57.
43. Ozer H, Cowens JW, Colvin M, Nussbaum-Blumenson A, Sheedy D. In vitro effects of 4-hydroperoxycyclophosphamide on human immunoregulatory T subset function. I. Selective effects on lymphocyte function in T-B cell collaboration. *J Exp Med*. 1982;155(1):276–90.
44. Luan Y, Edmonds ME, Woodruff TK, Kim SY. Inhibitors of apoptosis protect the ovarian reserve from cyclophosphamide. *J Endocrinol*. 2019;240(2):243–56.
45. Ohtani T, Nakamura T, Toda K, Furukawa F. Cyclophosphamide enhances TNF-alpha-induced apoptotic cell death in murine vascular endothelial cell. *FEBS Lett*. 2006;580(6):1597–600.
46. Andoh T, Goto M. Repeated topical paeoniflorin attenuates postoperative pain and accelerates cutaneous fibroblast proliferation in mice. *J Pharmacol Sci*. 2023;151(2):84–7.
47. Xu J, E XQ, Liu HY, Tian J, Yan JL. Angelica Sinensis attenuates inflammatory reaction in experimental rat models having spinal cord injury. *Int J Clin Exp Pathol*. 2015;8(6):6779–85.
48. Park CH, Noh JS, Tanaka T, Yokozawa T. Effects of morroniside isolated from Corni Fructus on renal lipids and inflammation in type 2 diabetic mice. *J Pharm Pharmacol*. 2010;62(3):374–80.
49. Sun FL, Wang W, Zuo W, Xue JL, Xu JD, Ai HX, et al. Promoting neurogenesis via Wnt/beta-catenin signaling pathway accounts for the neurorestorative effects of morroniside against cerebral ischemia injury. *Eur J Pharmacol*. 2014;738:214–21.
50. Zhang J, Wang H. Morroniside protects against chronic atrophic gastritis in rat via inhibiting inflammation and apoptosis. *Am J Transl Res*. 2019;11(9):6016–23.
51. Zhang JX, Wang R, Xi J, Shen L, Zhu AY, Qi Q, et al. Morroniside protects SK-N-SH human neuroblastoma cells against H₂O₂-induced damage. *Int J Mol Med*. 2017;39(3):603–12.
52. Chen H, McCaffery JM, Chan DC. Mitochondrial fusion protects against neurodegeneration in the cerebellum. *Cell*. 2007;130(3):548–62.
53. Lee S, Sterky FH, Mourier A, Terzioglu M, Cullheim S, Olson L, et al. Mitofusin 2 is necessary for striatal axonal projections of midbrain dopamine neurons. *Hum Mol Genet*. 2012;21(22):4827–35.
54. Parone PA, Da Cruz S, Tondera D, Mattenberger Y, James DI, Maechler P, et al. Preventing mitochondrial fission impairs mitochondrial function and leads to loss of mitochondrial DNA. *PLoS ONE*. 2008;3(9):e3257.
55. Boncompagni S, Rossi AE, Micaroni M, Beznoussenko GV, Polishchuk RS, Dirksen RT, et al. Mitochondria are linked to calcium stores in striated muscle by developmentally regulated tethering structures. *Mol Biol Cell*. 2009;20(3):1058–67.
56. Gao F, Reynolds MB, Passalacqua KD, Sexton JZ, Abuaita BH, O’Riordan MXD. The mitochondrial Fission Regulator DRP1 controls post-transcriptional regulation of TNF-alpha. *Front Cell Infect Microbiol*. 2020;10:593805.
57. Hu J, Zeng C, Wei J, Duan F, Liu S, Zhao Y, et al. The combination of Panax ginseng and Angelica Sinensis alleviates ischemia brain injury by suppressing NLRP3 inflammasome activation and microglial pyroptosis. *Phytomedicine*. 2020;76:153251.
58. Guo YJ, Pan WW, Liu SB, Shen ZF, Xu Y, Hu LL. ERK/MAPK signalling pathway and tumorigenesis. *Exp Ther Med*. 2020;19(3):1997–2007.
59. Yue TL, Wang C, Gu JL, Ma XL, Kumar S, Lee JC, et al. Inhibition of extracellular signal-regulated kinase enhances Ischemia/Reoxygenation-induced apoptosis in cultured cardiac myocytes and exaggerates reperfusion injury in isolated perfused heart. *Circ Res*. 2000;86(6):692–9.
60. Ji X, Liu X, Li X, Du X, Fan L. MircoRNA-322-5p promotes lipopolysaccharide-induced acute kidney injury mouse models and mouse primary proximal renal tubular epithelial cell injury by regulating T-box transcription factor 21/mitogen-activated protein kinase/extracellular signal-related kinase axis. *Nefrologia (Engl Ed)*. 2023.
61. Jia H, Dilger P, Bird C, Wadhwa M. IL-27 promotes proliferation of human leukemic cell lines through the MAPK/ERK Signaling Pathway and suppresses sensitivity to chemotherapeutic drugs. *J Interferon Cytokine Res*. 2016;36(5):302–16.
62. Ma Y, Liu W, Wang Y, Chao X, Qu Y, Wang K, et al. VEGF protects rat cortical neurons from mechanical trauma injury induced apoptosis via the MEK/ERK pathway. *Brain Res Bull*. 2011;86(5–6):441–6.

Publisher’s note

Springer Nature remains neutral with regard to jurisdictional claims in published maps and institutional affiliations.